https://doi.org/10.5194/hess-2019-541
Preprint. Discussion started: 24 October 2019

Hydrology and Earth System Sciences
Discussions
Open Access

Partitioning the forest water balance within a boreal catchment using sapflux, eddy covariance and process-based model

Nataliia Kozii[1], Kersti Haahti[2], Pantana Tor-ngern[3], Jinshu Chi[1], Eliza Maher Hasselquist[1], Hjalmar Laudon[1], Samuli Launiainen[2], Ram Oren[4], Matthias Peichl[1] Jörgen Wallerman[5], Niles J. Hasselquist[1*]

[1]Department of Forest Ecology and Management, Swedish University of Agricultural Science, Umeå, 90183, Sweden

[2]Natural Resources Institute Finland (Luke), Latokartanonkaari 9, 00790 Helsinki, Finland

[3]Department of Environmental Science, Chulalongkorn University, Bangkok, 10330, Thailand

[4]Nicholas School of the Environment, Duke University, Durham, 27708, North Carolina, USA

[5]Department of Forest Resource Management, Swedish University of Agricultural Science, Umeå, 90183, Sweden

**Correspondence to*: Niles Hasselquist (niles.hasselquist@gmail.com)

Abstract

In the hydrological cycle, water is lost from terrestrial ecosystems either laterally through stream runoff or vertically as evapotranspiration (ET) back to the atmosphere. Although it is well known that ET losses represents an important water loss pathway at local to global scales, the magnitude and relative importance of ET and its individual flux components varies considerable among different ecosystems. In this study, we combined empirical sapflux and eddy covariance measurements with estimates from a process-based model to partition the water balance in a boreal forested catchment. This study was conducted within the Krycklan Catchment, which has state-of-the-art infrastructure for hydrological measurements, thereby providing us the unique opportunity to compare the absolute and relative magnitude of ET and its flux components to other water loss pathways (i.e., stream runoff). During the growing season, ET was the major water loss pathway, representing *ca.* 85 % of the incoming precipitation and being roughly 7 times greater than stream runoff. Both the empirical results and model estimates suggested that tree transpiration (T) and canopy interception (IL) represented 45 % and 35 % of total ET loss; respectively, and thus together were responsible for 70 % of the water loss during the growing season. Understory evapotranspiration (ETu) was less important than T and IL during most of the study period, except for late autumn when ETu was the largest ET flux component. Overall, our study highlights the importance of trees in regulating the water cycle of boreal catchments, implying that forest management

impacts on stand structure as well as climate change effects on tree growth are likely to have large cascading effects on the way water moves through these forested landscapes.

1 Introduction

In the hydrological cycle, water enters terrestrial ecosystems mainly through precipitation. This water is lost either through surface runoff or evapotranspiration (ET) back to the atmosphere. At a global scale, ET losses can account for *ca*. 60 % of the annual terrestrial precipitation (Oki and Kanae, 2006). Yet the magnitude, as well as the relative importance, of ET varies considerably among different ecosystems (Peel et al., 2010). Understanding this variation in ET loss is crucial, as the difference between incoming precipitation and ET represents the available water to a hydrological system, which in turn has cascading effects on streamflow (Karlsen et al., 2016;Koster and Milly, 1997), groundwater recharge (Githui et al., 2012) and the ecosystem carbon cycle (Wang et al., 2002;Öquist et al., 2014).

For a long time, most hydrological studies have treated ET as a single water flux. However, ET represents two fundamentally different pathways of water loss from terrestrial ecosystems: (1) transpiration through stomata of plants and (2) evaporation from wet surfaces. These two different pathways are controlled in contrasting ways and to varying degrees by environmental factors and thus are likely to respond differently to climate change and land management practices. Specifically, transpiration occurs mainly during the vegetation season and is thus governed by plant physiological processes, whereas evaporation occurs throughout the year and is strongly controlled by vapor pressure deficit, surface wetness, and aerodynamic conductance (Stoy et al., 2006). Thus, quantifying the magnitude and drivers of transpiration and evaporation are crucial to better understanding the spatiotemporal variation of water fluxes in terrestrial ecosystems.

During the past decade, there has been increasing number of studies partitioning ET into transpiration and evaporation (see Schlesinger and Jasechko (2014)). Based on the isotopic composition of water (δ^2H and δ^{18}O) collected from large lakes, Jasechko et al. (2013) estimated that at a global scale transpiration represents 80 to 90 % of terrestrial ET. The high estimate of T/ET reported by Jasechko et al. (2013) has been strongly contested (Coenders-Gerrits et al., 2014), with a more conservative estimate of transpiration representing *ca.* 60 % of ET being more generally accepted (Schlesinger and Jasechko, 2014;Wei et al., 2017). Despite these recent advances in partitioning ET, most ecohydrological studies typically partition ET at the stand or plot scale without considering the broader hydrological cycle (e.g. Cienciala et al., 1997;Grelle et al., 1997;Schlesinger and Jasechko, 2014;Wang et al., 2017;Ohta et al., 2001;Iida et al., 2009;Hamada et al., 2004;Maximov et al., 2008;Warren et al., 2018). We are aware of only a few investigations that have provided a detailed water balance at the catchment scale (Sarkkola et al., 2013b;Telmer and Veizer, 2000), and thus we have little empirical data about how the amount of water that is lost via transpiration compares to other water fluxes (i.e., streamflow) in the terrestrial hydrological cycle.

Transpiration can be further partitioned into canopy tree transpiration and understory vegetation transpiration. Few studies have measured understory transpiration, yet the ones that have suggest that understory transpiration represents a small fraction of total transpiration (Kulmala et al., 2011;Palmroth et al., 2014) and is strongly dependent on canopy tree structure (Constantin et al., 1999;Baldocchi et al., 1997;Domec et al., 2012). Similarly, total evaporation can be partitioned into canopy interception losses (IL) and evaporation from the forest floor. At a global scale, roughly 20 % of incoming precipitation is lost via IL (Wang et al., 2007) and in many forested ecosystems IL represents a substantial portion of total evaporation (Barbier et al., 2009;Gu et al., 2018). By separating transpiration and evaporation into their different flux components, it is possible to directly assess the relative importance of trees (i.e., canopy transpiration + IL) to other water loss pathways and in turn determine the important role trees play in the terrestrial hydrological cycle.

There are numerous different approaches and methodology to partition ET into its different flux components (Kool et al., 2014). One approach is to use a combination of eddy-covariance methods to estimate ET and sap flow sensors to separately estimate transpiration in the dominant canopy trees (Mitchell et al., 2009;Cavanaugh et al., 2011), although this approach often ignores sub-canopy vegetation. Combining this approach with the placement of rain gauges under the forest canopy and in open sky it is also possible to estimate IL and its relative importance to total ET losses. With recent advances in techniques and instrumentation it is now also possible to use the stable hydrogen and oxygen isotopes (δ^2H and δ^{18}O) of liquid water to partition ET (Evaristo et al., 2015;Good et al., 2014;Sutanto et al., 2014). In addition to these empirical approaches, there are a number of different process-based models that can be used to partitioning ET into its different flux components (Sutanto et al., 2014;Stoy et al., 2019). Each of these different approaches have their advantages and disadvantages and moreover it has been shown that the relative contribution of ET flux components differs depending on the approach used (Schlesinger and Jasechko, 2014). It has therefore been highlighted that the use of multiple methods is desirable to more accurately partition ET into it individual flux components (Stoy et al., 2019).

In this study, we use a combination of empirical data derived from eddy-covariance and sapflux measurements as well as rain gauges collecting open sky and throughfall precipitation to partition ET into its individual flux components during the growing season in a boreal catchment. Additionally, we used a multi-layer, multi-species soil-vegetation-atmosphere transfer model (APES model based on Launiainen et al., 2015) as another independent approach to partition ET. In doing so, the main objective of this study was to *i*) constrain the absolute and relative magnitude of ET flux components by using both empirical data and model simulations and *ii*) to explore how they vary during the course of the growing season. This study was conducted within the Krycklan Catchment, which has state-of-the-art infrastructure for hydrological measurements, thereby providing us the unique opportunity to compare different ET fluxes to other water loss pathways (i.e., streamflow) and to directly assess the important role trees play in the boreal hydrological cycle.

2. Material and Methods

2.1 Study site

The study was conducted in the 14 ha subcatchment C2 (64.26° N, 19.77° E) within the 64 km^2 Krycklan Catchment Study area (Laudon et al., 2013) in northern Sweden (Fig. 1). The Krycklan Catchment Study area is unique as it is one of the oldest long-term catchment monitoring sites in northern latitudes with continuous hydrological and meteorological measurements dating back to the early 1980s. The 30-year mean annual temperature in Krycklan (1986-2015) was 2.1° C; with highest mean monthly temperature in July and lowest temperature in January (14.6°C and -8.6°C; respectively). The mean annual precipitation was 619 mm, with the majority (ca. 60%) falling in the form of rain. Soils within the C2 are dominated by glacial till (84%), predominately of stony, sandy texture on gneiss and granite. There is considerable variation in the thickness of the humus layer, yet the average is 8 cm (Odin, 1992). The average slope is 6% and the outlet of the C2 subcatchment is located at 243 m a.s.l.

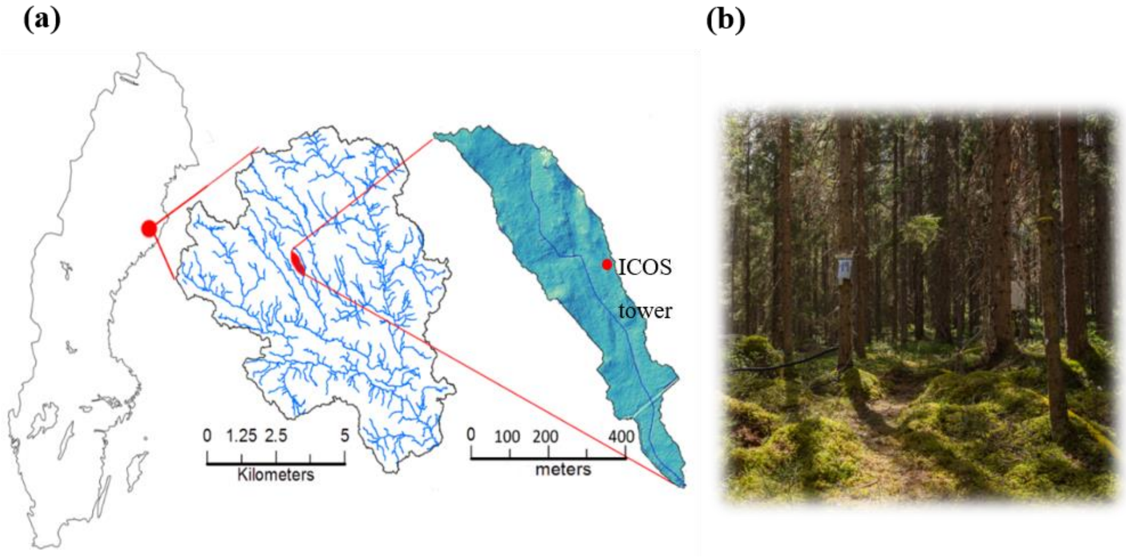

Figure 1. Location of the studied C2 subcatchment within the Krycklan Catchment in northern Sweden (a) and a picture of forest stand and rich understory vegetation that is characteristic of the C2 subcatchment (b).

The catchment is characterized by an old (>100 yr.) mixed forest stand of *Picea abies* (61 %), *Pinus sylvestris* (34 %), and *Betula* (5 %) (Laudon et al. 2013). The understory consists of a rich layer of bilberry (*Vaccinium myrtillus*), lingonberry (*Vaccinium vitis-idaea*), and mosses (*Pleurozium schreberi* and *Hylocomium splendens*). Similar forest stands extend to the east and west of the C2 subcatchment boundaries by several hundred meters. Within the C2 subcatchment, there is also the Integrated Carbon Observation System (ICOS) Svartberget ecosystem-atmosphere station which provides data on greenhouse gas, water and energy fluxes as well as meteorological, vegetation and soil environmental variables (www.icos-sweden.se/station_svartberget.html). Our study period was from July to October 2016 which corresponded to the snow free growing season, spanning from after the spring flood until leaf senescence for deciduous species. The 2016 year was a typical year in terms of precipitation and stream runoff (Fig. S1).

2.2 Empirical measurements of the water balance components

To quantify water balance components at the catchment scale, we combined multi-scale measurements of vertical and lateral water fluxes made within the C2 subcatchment. The underlying assumption in our analysis is that forest stand characteristics are uniform across and beyond the C2 subcatchment, which allows us to directly compare water fluxes per unit area regardless of the spatial scale the measurements represents: stand vs. catchment.

Precipitation (P) and other environmental data at 30 min temporal resolution were obtained from the ICOS portal, Svartberget station (http://www.icos-sweden.se/data.html). For this study we used data of daily mean air temperature, relative humidity, wind speed, total precipitation, atmospheric pressure, incoming short and long-wave radiation, photosynthetic active radiation (PAR), as well as soil temperature and moisture measured at 0.05 m depth. Daily stream runoff (Q) was calculated as ratio of daily discharge, obtained from the Svartberget data portal (https://franklin.vfp.slu.se/), and catchment area. Changes in soil storage (ΔS) were not empirically measured in this study.

Evapotranspiration (ET) data were derived from the ICOS-Svartberget eddy covariance (EC) system installed at 32.5 m above the ground. The setup consists of a 3D ultrasonic anemometer (uSonic3 Class-A, METEK Meteorologische Messtechnik GmbH, Germany) for measuring wind components (*u*, *v*, *w*) and a closed-path infrared gas analyzer (LI-7200, LI-COR Biosciences, USA) for measuring CO_2 and H_2O concentrations. The EC raw data were recorded at 10 Hz frequency and 30-min fluxes were processed in the EddyPro® software (version 6.2.0, LI-COR Biosciences, USA) according to common settings described in details in Chi et al. (2019). Briefly, the ET data were computed as a covariance of vertical wind speed (*w'*) and H_2O concentration (*q'*) for each 30-min period and corrected for water vapor storage in the air volume between the measurement height and the forest ground:

$$ET = \overline{w'q'} + \int_0^h \overline{\rho_d} \frac{\partial \bar{q}}{\partial t} \delta z \qquad (1)$$

where h = 32.5 m, t = 30 min, $\overline{\rho_d}$ is dry air density, q is profile measurements of water vapor concentrations at different height (z) from 4.2 to 30 m above the ground. ET data were then filtered for the non-ideal conditions for EC measurements, i.e. non-stationarity, wind distortion, power failure, as well as site maintenance activities (Chi et al., 2019). The potential advection effects on ET data were detected using the turbulence intensity parameters (Wharton et al., 2009) and data were discarded when advection was no longer negligible. Gaps in the half-hourly ET data were filled using the REddyProcWeb online tool

(Wutzler et al., 2018). Based on the Kljun footprint model (Kljun et al., 2015), the EC footprint (90 %) covers a measurement area of ~0.5 km^2 with a mean upwind fetch of ~400 m surrounding the tower. The uncertainty in the EC-based ET was estimated by the Monte Carlo simulation (Richardson and Hollinger, 2007).

Evaporation of intercepted water from tree canopy was estimated based on canopy interception losses (IL) and was determined by subtracting throughfall (TF) from open sky precipitation (P): IL = GP – TF. Measurements of TF were made 1 km from the study subcatchment by installing 25 rain gauges to measure throughfall in a similar mature mixed coniferous forest stand. The design of rain gauges followed WMO (Bidartondo et al., 2001) requirements, which included a stable rim with sharp edge, orifice area of 200 cm^2, hydrophobic plastic material and a narrow entrance to the receiving container to prevent evaporation. To test custom made gauges, three of them were installed next to a standardized precipitation collector Geonor T200BM (Geonor Inc., New Jersey, USA) at the Svartberget field station for the entire period and the difference in captured rain was always less than 3%. Measurements of TF were made between the beginning of July and the end of October 2016, at an event-based frequency. The IL (mm) for a single rain event was estimated as weighted average from the 25 throughfall gauges. Weighting was based on spatial forest canopy density data acquired by airborne laser scanning (ALS), using a canopy metric calculated from all canopy height measurements within a two-meter horizontal distance of the collector, and frequency distribution of that canopy metric within the C2 subcatchment. The canopy metric used for this procedure was the median of the absolute deviation of ALS height measurements from the overall median height (ElvMADmedium). This particular metric was chosen from the set of metrics calculated by the FUSION software (McGaughey, 2012) because it had the highest correlation with measured seasonal interception loss. To eliminate influence of potential difference between open sky precipitation within the C2 subcatchment and sampling plot on the final results, at the end of sampling campaign, we estimated the fraction of seasonal interception loss (IL_f=1-TF/GP) and multiplied that value by cumulative precipitation at the study catchment. To quantify the uncertainty of the event-based IL estimated from measurement, we grouped the gauges into 5 groups based on the ElevMADmedian canopy metric and calculate standard deviation for each group and event.

Canopy transpiration (T) was estimated using sap flux measurements. Within the EC footprint area, we selected three locations (hereafter referred to as nodes) to measure canopy transpiration (Fig. S2). Within each node (25 m radius), we selected 20 trees (10 *Pinus sylvestris* and 10 *Picea abies*) that represented the diameter distribution of the entire C2 subcatchment forest stand. Although *Betula spp.* is also present within the C2 subcatchment, they contribute less than 5% of the basal area and we therefore focused on the two dominant conifer species (Laudon et al., 2013).

Sap flux density (J_S, g $m^{-2}_{sapwood}$ s^{-1}) was measured at breast height (1.3 m above ground) using custom-made heat dissipation-type sap flow sensors (Granier, 1987). Each pair of sensors consisted of a heated and non-heated probe made from 19-gauge hypodermic needles with metallic, sensing parts cut into 20 mm length. These sensors were installed on the selected trees with 10-15 cm spacing between probes and all sensors were covered with reflective insulation to reduce external temperature influences. To account for radial (Phillips et al., 1996;Ford et al., 2004;Oishi et al., 2008) and azimuthal (Oren et al., 1999;Lu et al., 2000;James et al., 2002;Tateishi et al., 2008) variation in J_S, we installed sensors in the north, east, south and west sides of the stems in 6 of the selected trees from all nodes (n = 3 per species). We also installed sensors at four 20 mm interval depths from the inner bark (i.e., 0-20 mm, 20-40 mm, 40-60 mm and 60-80 mm) in a subset of tree species. Data of temperature difference between the two probes were collected as 30-minute averages of voltage difference (ΔV, mV) using a data logger (CR1000, Campbell Scientific, Logan, UT, USA) which was set to record data every 30 s. The collected data were converted to J_S using the empirical equation (Granier, 1987)

$$J_S = 118.99 \times 10^{-6} \times \left(\frac{\Delta V_m - \Delta V}{\Delta V} \right)^{1.231} \quad (2)$$

where ΔV_m is the maximum voltage difference under zero flow conditions which occur at night and when vapor pressure deficit is low. We employed the Baseliner program version

4.0 (Oishi et al., 2016) to convert the ΔV data to J_S. This accounts for nocturnal fluxes resulting from nighttime transpiration and water recharge in stems by selecting the highest daily ΔV to represent ΔV_m. The selection criteria for determining ΔV_m were conditions when (1) the average, minimum 2-hour vapor pressure deficit is less than 0.02 kPa, thus ensuring negligible transpiration and (2) the standard deviation of the four highest values is less than 0.5 % of the mean of these values, therefore ensuring that water storage change above the sensor height is negligible compared to J_S.

To determine daily canopy transpiration (T, mm d^{-1}), we first integrated J_S over 24 hours as daily J_S (J_{SD}, g $cm^{-2}{}_{sapwood}$ d^{-1}) to avoid issues related to tree water storage and measurement errors (Phillips and Oren, 1998). Then, we tested J_{SD} variations within sapwood areas in the trees and found insignificant azimuthal variation ($p \geq 0.23$) but significant variation along sapwood depth ($p < 0.001$). Accordingly, we performed a scaling based on the radial variation of J_{SD}. First, we evaluated the relationship between the outermost J_{SD} at 0-20 mm ($J_{SD,0\text{-}20mm}$) sapwood depth and DBH and found no significant effects of stem size on $J_{SD,0\text{-}20mm}$ in either species ($p \geq 0.1$). Therefore, we averaged $J_{SD,0\text{-}20mm}$ across all sampled trees and used the data for scaling. Next, we calculated the ratios between J_{SD} at inner sapwood depths (i.e., 20-40 mm, 40-60 mm and 60-80 mm) and $J_{SD,0\text{-}20mm}$ during the study period. Because there was no significant relationship between the ratios and stem size ($p \geq 0.16$), we averaged the ratios across all trees for each species in each day and used the daily specific ratios between J_{SD} in the inner sapwood depths and the outermost J_{SD} ($J_{SD,0\text{-}20mm}$) for scaling. Sapwood area (A_S, cm^2) for each tree species (*P. sylvestris* and *P. abies*) was estimated from allometric equations derived from > 20 tree cores taken at breast height for each tree species in 2017. Tree cores were taken from individual trees representing the full range of stem diameter distribution at the site and stained with alcohol iodine solution (Eades, 1937) to record the depth of active sapwood thereby allowing the estimation of A_S of all trees. For scaling, we first estimated weighted average J_{SD} of each species ($J_{SD,species}$; g cm^{-2} d^{-1}) using data from the three nodes by

$$J_{SD,species} = \frac{\sum_{i=1}^{5} J_{SD,i} \times A_{S,i}}{A_{S,all}} \qquad (3)$$

i is the sapwood depth from the inner bark; i.e., 0-20 mm, 20-40 mm, 40-60 mm, 60-80 mm and >80 mm, $J_{SD,i}$ is the average daily sap flux density for each layer and calculated as the product of the averaged ratios and $J_{SD,0\text{-}20mm}$, $A_{S,i}$ is sapwood area of layer i and $A_{S,all}$ is the total sapwood area of all trees of the species from all nodes. Then, using this weighted average J_{SD} by species, the canopy transpiration of the C2 subcatchment (T, mm d^{-1}) was estimated using sapwood area index (SAI, $m^2_{sapwood}\, m^{-2}_{ground}$) of each species, which was derived from data from seven permanent forest inventory plots located within the C2 subcatchment.

$$T = 10 \times (J_{SD,pine} \times SAI_{pine} + J_{SD,spruce} \times SAI_{spruce}) \qquad (4)$$

where 10 is the unit conversion factor. Regarding methodological considerations, the most common criticism of the heat dissipation method for sap flux measurement, is that it underestimates the flux (Sun et al., 2012;Steppe et al., 2010). However, according to the analysis of 54 data from global pine forests in Tor-ngern et al. (2017) estimates from other sap flux measurement methods showed no particular bias from those with the heat dissipation one as used in this study. In addition, it has previously been shown that radial variation of sap flux density and tree size were more important than species in scaling from single-point sap flux measurements to stand transpiration (Hernandez-Santana et al., 2015), both of which were considered in our analysis. In this study, uncertainty of daily transpiration is represented by standard deviation of T within the seven permanent forest inventory plots.

2.3 Modeling ET partitioning

We also partitioned ET using a detailed ecohydrological model. We used a slightly modified version of the soil-vegetation-atmosphere transfer model APES (Launiainen et al., 2015) which simulates water, energy, and carbon dioxide (CO_2) fluxes in a forest ecosystem in the vertical dimension. The forest is described by a multi-layer, multi-species tree stand, understory vegetation, and a bryophyte layer on the forest floor and thus allows partitioning water fluxes between canopy layers and species. The heat and water fluxes within the soil profile were not solved in this study, instead we used measured soil moisture and soil temperature at the depth of 0.05 m as lower boundary conditions.

As forcing variables, the model uses time-averaged (here ½ hourly) meteorological variables at a reference level above the canopy. These include P, downwelling longwave radiation, direct and diffuse photosynthetically active and near-infrared radiation, wind speed (or friction velocity), atmospheric pressure, air temperature (T_{air}), and mixing ratios of H_2O and CO_2. Forcing data were taken from the Svartberget ICOS station using additional meteorological measurements from another ICOS station Degerö (at 15 km distance) to fill missing values. For precipitation the Degerö readings were corrected to match the daily precipitation measured at another station (at 1 km distance) before using them for gap filling.

In APES, the canopy is considered as a layered porous media characterized by leaf-area density (LAD) distribution. The model solves the transfer and absorption of shortwave and longwave radiation (Zhao and Qualls, 2005, 2006) and the transport of scalars (T_{air}, H_2O, CO_2) and momentum among canopy layers (here n=100). Partitioning of rainfall between interception and throughfall, as well as the energy balance of wet leaves is also solved for each canopy layer (Watanabe and Mizutani, 1996). The canopy LAD distribution is further divided into LAD distributions for each plant type (e.g. main tree species and understory vegetation). Each plant type is characterized by physiological properties describing phenology, photosynthetic capacity, and stomatal conductance. Leaf gas and energy exchange is calculated separately for sunlit and shaded leaves of each plant type using well-established coupled photosynthesis–stomatal conductance theories (Medlyn et al., 2011;Farquhar et al., 1980) and leaf energy balance. A separate forest floor component describes water, energy and CO_2 dynamics in the bryophyte layer (Kieloaho and Launiainen, 2018;Launiainen et al., 2015).

To model the ET components, we established LAD distributions for the main tree species (*Picea abies*, *Pinus sylvestris*, and *Betula pendula*) based on stand inventories from seven forest plots (10 m radius) within the C2 subcatchment. The frequency distributions of diameter at breast height for each species were derived into LAD distributions based on the models by Marklund (1988), Näslund (1936) and Tahvanainen and Forss (2008), and the specific leaf area values reported by Harkonen et al. (2015). The total one-sided leaf area index (LAI_{tot}) was scaled to match the LAI derived from the empirically measured LAI_{Licor} with LAI-2200C Plant Canopy Analyzer (LAI_{Licor} = 2.75) using a correction of 1.6–1.9 (Stenberg et al., 1994), resulting in LAI_{tot} = 4.4-5.2 m^2 m^{-2} (Selin, 2019). The resulting normalized LAD distributions are shown in Fig. S3. In the simulations understory LAI was set to LAI_{under} = 0.4–0.8 m^2 m^{-2}, and the bryophyte layer was characterized as feather moss. A full list of model parameters can be found in supplementary Tables S1 and S2.

We simulated the period from May to October 2016, and included parameter uncertainty through parameter ranges for LAI_{tot}, LAI_{under}, maximum carboxylation rate

(V_{cmax}) at 25°C and interception capacity (see Tables S1 and S2). To assess model performance, model results were evaluated at ½ hourly time interval against ecosystem fluxes (net shortwave and longwave radiation, latent heat, sensible heat and gross primary productivity) observed at the ICOS-Svartberget EC tower (Chi et al., 2019). Performance test against the simulation results for the center of the parameter space showed a good agreement between modelled and measured variables (Fig. S4). Net shortwave and longwave radiation were predicted with good accuracy, which is crucial for further modeling steps. Sensible heat flux was slightly overestimated and latent heat flux slightly underestimated. Model results of ET components were further analyzed on a daily or rain event based time interval and compared against corresponding estimates derived from empirical measurements.

3 Results

Meteorological conditions during the snow free vegetation season of 2016 (Fig. 2) were similar to long term averages. The highest daily mean temperatures were in the middle of July (ca. 20 °C) followed by a gradual decrease to around 0 °C at the end of October. As observed for air temperature, photosynthetically active radiation (PAR) peaked at the end of July and then decreased to less than 20 W m^{-2} at the end of October. During the study period daily vapor pressure deficit (VPD) ranged between 0 and 1.5 kPa, with a notable peak in the middle of July, which also corresponded to a peak in air temperature. Total precipitation over the study period was 226 mm, with a strong peak in early August and another at the end of September. These events are also observed as peaks in stream runoff (Fig. 2c).

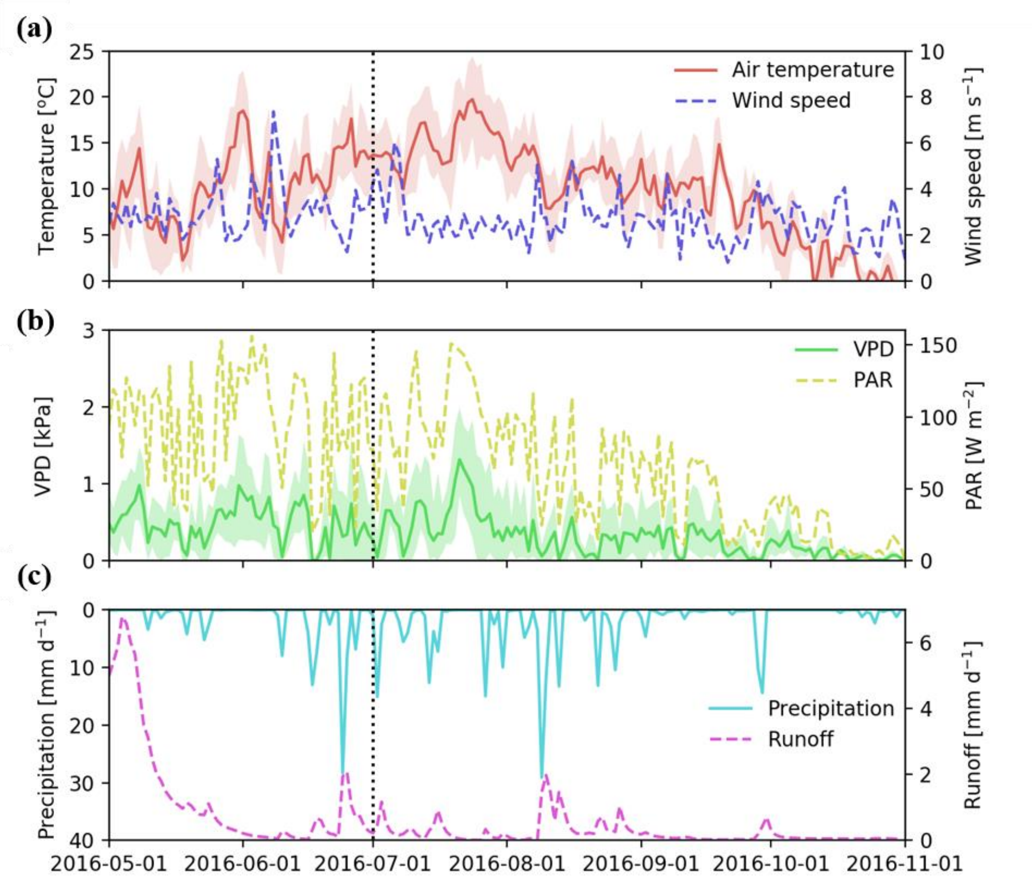

Figure 2. Mean daily hydro-meteorological variables at the Krycklan catchment during the
355 2016 growing season: air temperature and wind speed (a); vapor pressure deficit, VPD and photosynthetically active radiation, PAR (b); precipitation and stream runoff (c). Beginning of study period is marked with a vertical dotted line. Shaded areas for air temperature and VPD show minimum and maximum values during a day.

https://doi.org/10.5194/hess-2019-541
Preprint. Discussion started: 24 October 2019

3.1 Daily variability of ET and its components

Daily ET over the study period varied between 0 and 4 mm d^{-1} depending on the weather conditions (Fig. 3a). Except for the very short period following a 29 mm rain event on August 9, ET was always higher than Q. In general, there was good agreement between empirical and modeled estimates of ET ($R^2 = 0.79$; $P < 0.001$; Fig. 3a). Yet during a one-week period in July modeled estimates of ET were 30 % higher than measurement ET, which also corresponded to the time period of high IL (Fig. 3d).

The amount of water loss via T was substantial, and during 88% of the study period was higher than Q (Fig. 3b). Maximum daily values of T were reached during the latter half of July and occasionally exceeded 2 mm d^{-1} (Figure 3b). During summer months (JJA) and the first half of September, daily T was on average 0.93 mm d^{-1} but later substantially decreased to <0.2 mm d^{-1}. Overall, modelled estimates of T were tightly correlated with T based on sap flow measurements ($R^2 = 0.89$; $p < 0.001$), although the patterns of modelled and measured T diverged during a one-week in July (Fig. 3b).

Total evaporation together with understory transpiration (IL + ETu) had the highest variability (Fig. 3c) mainly because it includes interception evaporation (Fig. 3d) which is related to the frequency of rain events and only secondarily to other weather conditions like temperature or VPD (Fig. 3d). Modeled IL + ETu followed similar pattern to observed, which here is computed as a residual of ET and T (Fig. 3c). During rainy periods total evaporation exceeded T while the opposite was true for rain-free periods, e.g. during the second part of July the contribution of T to total ET was close to 80 %.

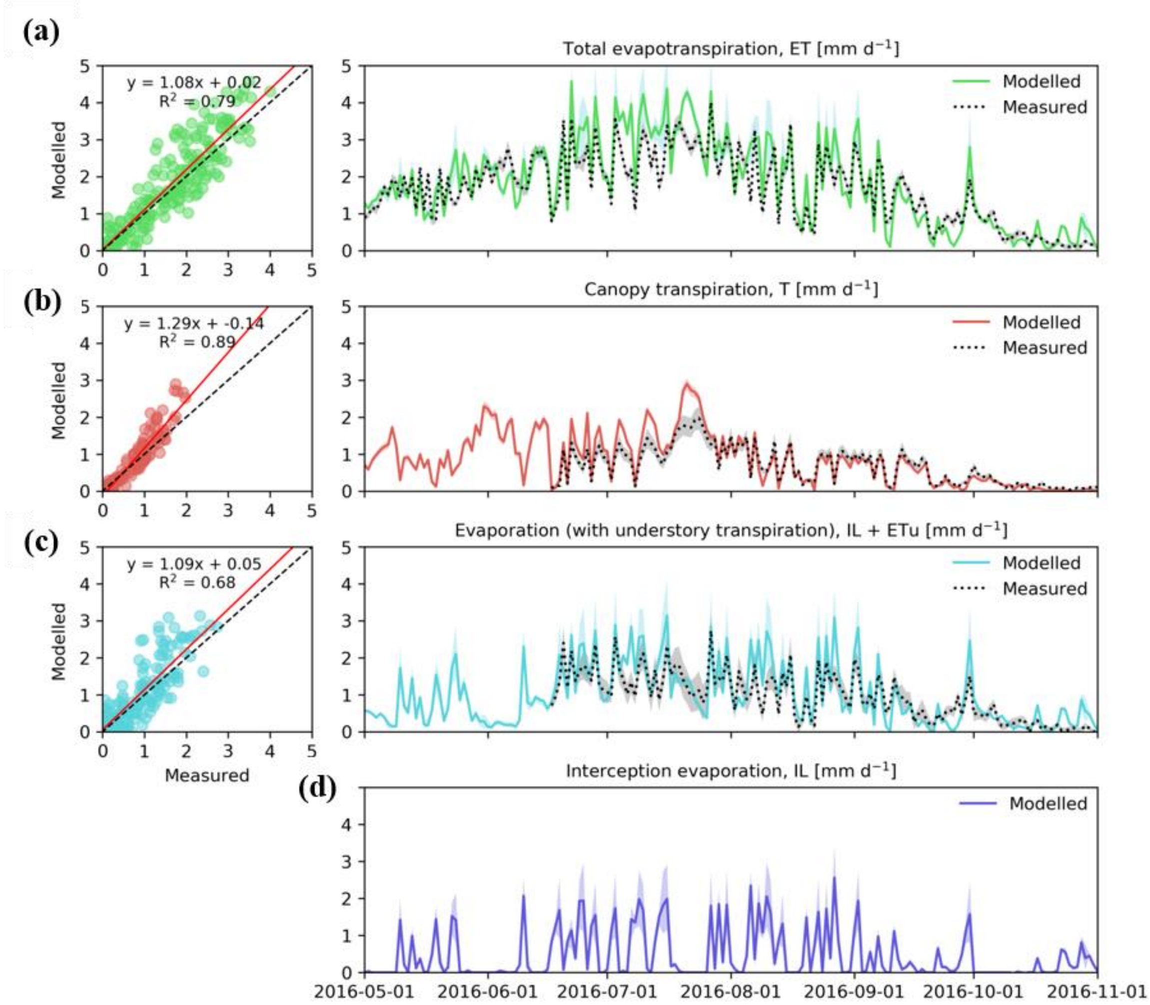

380

Figure 3. Evapotranspiration (a) and its component flux components: canopy transpiration, T (b), total evaporation with understory transpiration, IL + ETu (c) and canopy interception evaporation, IL (d) in a boreal forest catchment during the 2016 growing season. Small panels on a left side show correlation between daily modelled and measured values. Colored shaded areas show simulation results for whole parameter space and gray shaded areas
385 represents uncertainty in measurements.

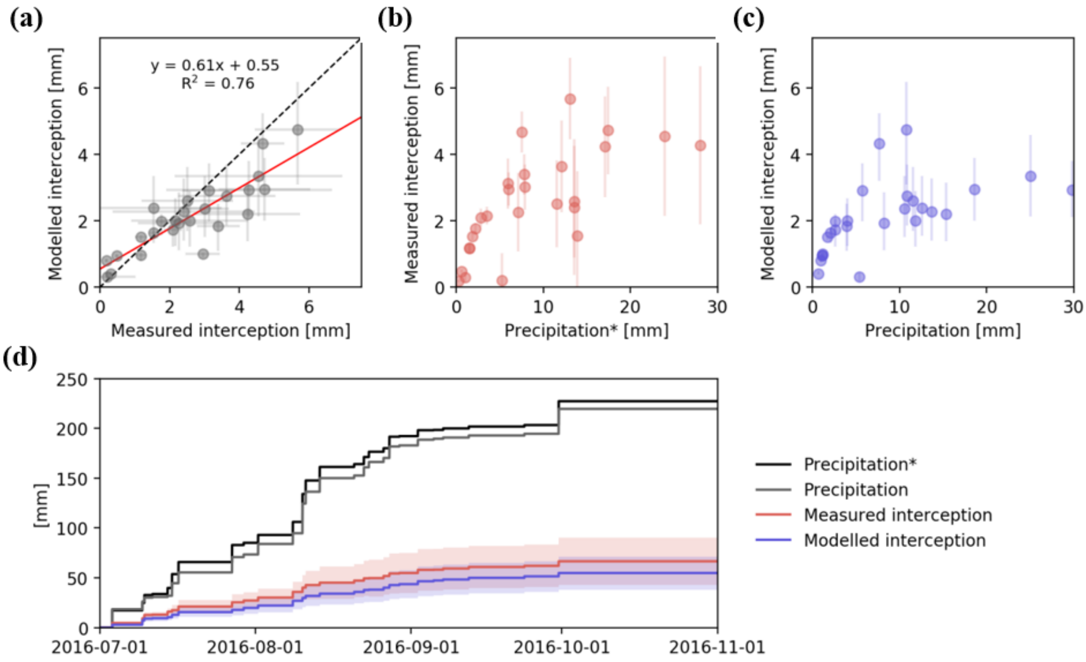

Figure 4. Comparison of measured and modelled event-based interception (IL) (a), relationship between precipitation and measured interception (b) and modelled interception (c). Cumulative plot of precipitation and interception based on the two different approaches (d). Error bars and shaded areas show simulation results for whole parameter space and uncertainty range in measurements. * refers to precipitation measured in open area at the same location as throughfall (see methods section).

Comparison of IL obtained by empirical measurements and modeling on event based time scale, which is the minimum temporal scale allowed by empirical sampling, showed high correlation, R^2=0.76 (Fig. 4a). However, modelled IL values were higher than measured for small rain events whereas the opposite was true for large rain events (Fig. 4a).

Uncertainty of both measured and modelled IL increased with the amount of precipitation (Fig. 4b, c). It is worth noting that precipitation used as reference for the throughfall measurements was from an open area close to the throughfall collectors, not from the ICOS station where precipitation was used in the model forcing. The difference in total precipitation from these two different sources was 7 mm, or 3 % over the entire study period (Fig. 4d).

3.2 Water balance and ET partitioning

During the growing season, the C2 subcatchment received 226 mm of precipitation and released only 28 mm of water as a stream runoff (Q). Based on EC measurements, ET represented 86 % of precipitation during the study period (194 ± 16 mm), which was similar to model estimated that showed 96 % of precipitation (217 ± 18 mm) was lost via ET during the study period (Fig. 5). When partitioning ET, it was found in both approaches that tree canopy transpiration (T) represents the largest flux of ET (44 % based on empirical measurements and 41 % based on model prediction). The amount of water lost via IL represents roughly 34 % and 28 % of total ET for the measured and modeling approach, respectively. When combining T and IL, trees were responsible for 78 % of ET when using empirical data and 69 % based on the model approach. Estimates of the relative importance of ETu was slightly higher when using the modeling approach compared to measure estimated (31 % and 22 %; respectively). Higher estimates of the relative importance of ETu in the modeling approach may be the result of reduced IL in the model compared to what was measured.

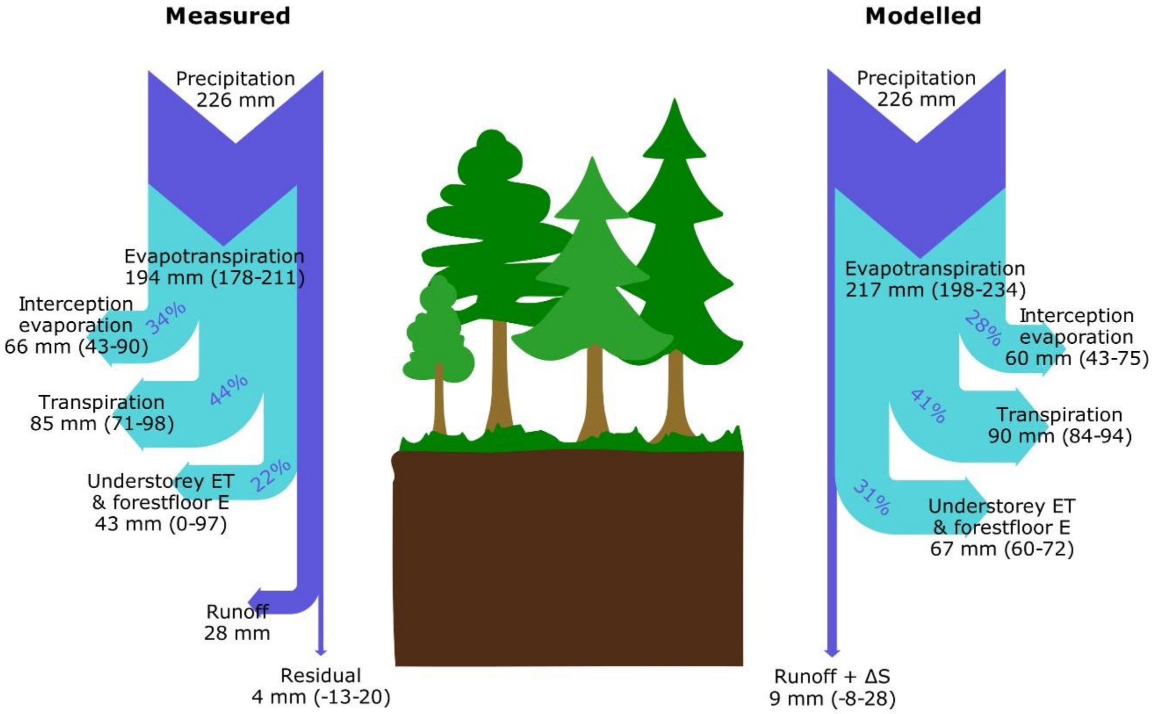

Figure 5. Partitioning of water fluxes based on empirical measurements (left side) and model simulation (right side) in a small coniferous boreal catchment during the 2016 growing season (July-October). Values for each flux component are presented as averages with upper and lower boundaries in parenthesis.

4. Discussion and Conclusion

In this study, we used both empirical measurements and a process-base model to partitioning ET into its individual flux components and assessed how these different fluxes varied during the course of the growing season in a northern boreal catchment. Both the empirical results and model estimates highlighted the importance of ET losses during the growing season, with ET representing *ca.* 85 % of the incoming precipitation during the study period. Moreover, the results demonstrated that canopy trees are the main driver of ET losses, as canopy transpiration (T) together with canopy interception losses (IL) represented 69-78 % of ET depending on the approach used. Being able to comparing the amount of water lost via different ET flux components to other water loss pathways within the subcatchment further emphasizes the important role canopy trees play in the hydrological cycle during the growing season and stresses the need to better understand the effect of trees on the catchment-scale water budget in response to forest management practices and a changing climate.

It is well known that there is strong seasonal variation in the relative importance of different water loss pathways in northern latitude catchments, with stream runoff being the main water loss pathway during snow melt in spring. Within the Krycklan Catchment, roughly 40 % of annual stream runoff occurs as a response to snowmelt (Ågren et al., 2012), when trees are relatively inactive (Tor-Ngern et al., 2017). In contrast, in this study we found that ET becomes the dominant water loss pathway after spring flood has ceased, and became

https://doi.org/10.5194/hess-2019-541
Preprint. Discussion started: 24 October 2019

seven times greater than stream runoff during the growing season (Fig. 2c, 3a). Moreover, the amount of water lost via ET during a three-week period in the middle of the growing season was comparable to the amount of water lost through stream runoff during spring peak flow (59.3 and 89.3 mm; respectively). Such asynchrony in relative importance of different water loss pathways might be even more pronounced in a future climate when higher air temperatures and less frequent, albeit more intense, precipitation events can be expected (IPCC, 2018). One future scenario is earlier snow melt, because of higher air temperatures (Byun et al., 2019), which would result in more water being lost as stream runoff thereby reducing the annual amount of water available for tree growth during the growing season (Barnett et al., 2005). In our study, combining precipitation with modelled estimates of ET and measured stream runoff results in a negative water balance (P < ET+Q) during the growing season. This is in agreement with other studies in boreal forests that have found a negative water balance during the growing season (Sarkkola et al., 2013b;Wang et al., 2017) which, in turn, could have cascading effects on forest productivity (Barber et al., 2000;Silva et al., 2010), tree mortality (Peng et al., 2011) and the overall carbon balance in boreal forests (Ma et al., 2012).

Our results further suggest that transpiration was the largest individual water flux during the growing season, representing *ca.* 40 % of incoming precipitation. Our cumulative T estimates during the study period (85-90 mm) was similar in magnitude to what has been observed in other boreal forests (e.g. Sarkkola et al., 2013b;Grelle et al., 1997). When compared to ET, T represented *ca.* 45 % of total ET loss (Fig. 5), which is consistent with other studies in boreal forests that have spanned between 39-85 % (39-48 % - Sarkkola et al. (2013b), 45-85 % - Cienciala et al. (1997), 47 % - Wang et al. (2017), 54 % - Ohta et al. (2001), 65 % - Grelle et al. (1997)). Meanwhile, our estimate of the relative importance of T to total ET, is slightly lower than the global average of ca. 60 % (Schlesinger and Jasechko, 2014;Wei et al., 2017). However, it is known that the ratio of T/ET varies considerably among different ecosystems as well as within the same ecosystems (Evaristo et al., 2015;Wei et al., 2017;Peel et al., 2010). Such variation in T/ET may be the result of differences in study location and duration, its spatial scale, forests stand structure, climatic conditions as well as the method used (Schlesinger and Jasechko, 2014). It is important to point out that the two approaches (*i.e.*, empirical measurements and modelling) gave similar estimates of T, both in term of overall magnitude (Fig. 5) and seasonal dynamics (Fig. 3b), thereby giving us confidence in our measurements of T.

There was good agreement on cumulative IL between empirical measurements and model estimates (66 and 60 mm; respectively), which corresponded to *ca.* 30 % of incoming precipitation during the study period. The importance of IL is however not surprising since Barbier et al. (2009) has previously shown that IL accounts for more than 30 % of seasonal precipitation in a wide range of temperate and boreal coniferous forest stands. When compared to other ET flux components, IL was the second largest ET flux component, representing *ca.* 35 % of total ET. In our study, IL was calculated for each rain event and it is important to point out that the fraction of P lost via IL (*i.e.*, IL/P) during a single rain event varies in response to the magnitude and intensity of P (Gash, 1979;Linhoss and Siegert, 2016;Rutter et al., 1971;Zeng et al., 2000). The highest IL/P are expected to occur during light rainfall events in a dry canopy, whereas IL/P decreases with increasing rain amount and intensity as well as when water storage capacity in the canopy is reduced by intercepted water from previous precipitation events. Given the strong interactions between the amount and intensity of P and IL, projected climate change in northern latitude ecosystems (IPCC, 2014) could drastically affect the amount of water lost via IL that, in turn, could strongly affect the amount of water available to plants, stream runoff and other downstream processes.

Understory evapotranspiration (ETu) represented 20 to 30 % of total ET depending on the method used, which is consistent with other studies in boreal forests where seasonal ETu/ET has been shown to range between 10 % and 50 % (Constantin et al., 1999;Iida et al., 2009;Kelliher et al., 1998;Suzuki et al., 2007;Launiainen et al., 2005;Launiainen, 2010). Although ETu was in general less important than T and IL during the entire study period, it is worth pointing out that ETu was the largest ET flux component in late autumn when the amount of water lost via T in canopy trees is reduced. Using the APES model we were able to further partition ETu into forest floor evaporation and understory transpiration. During the study period, cumulative water loss via forest floor evaporation was 57 mm, representing 85 % of total ETu, suggesting that evaporative water losses from the moss layer may play an important role in the boreal hydrological cycle, especially in late autumn (Bond-Lamberty et al., 2011;Suzuki et al., 2007). However, it is worth pointing out that ETu was the component 510 flux that showed the greatest difference between the two approaches, which stress the need for additional studies to better quantify ETu and its individual flux components.

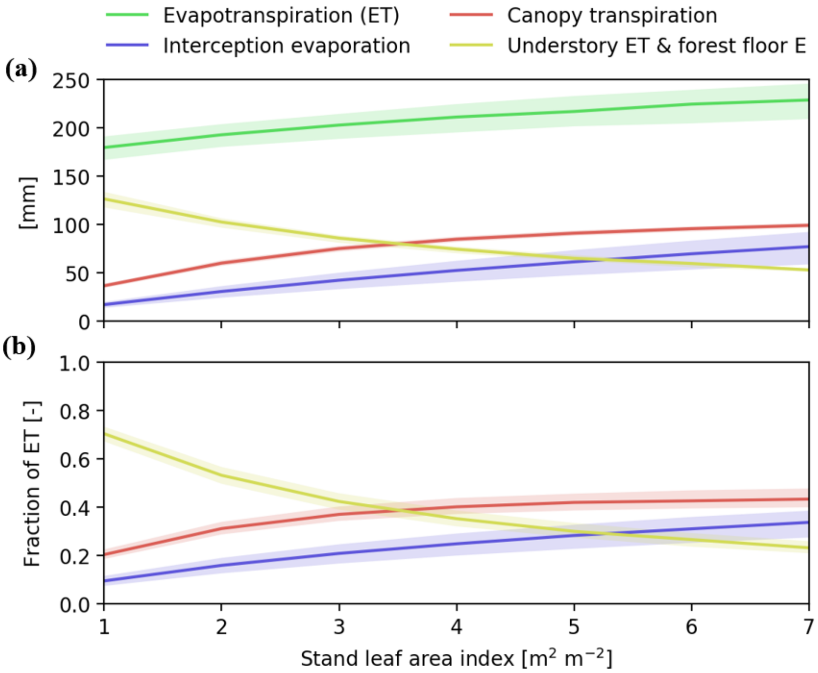

Figure 6. Modelling results for evapotranspiration and its components during July-October 515 2016 as a function of stand leaf area index in absolute amounts (a) and as a fractions of ET (b).

By combing T and IL, we are able to show that trees are directly responsible for *ca*. 70 % of water losses from a northern boreal catchment during the snow free growing season. Similarly, Gu et al. (2018) reported that T and IL together represent 55 to 83 % (average 63 %) of total ET across a range of needle-leaved evergreen forests in the boreal and temperate region. Taken together, there is increasing evidence highlighting the important role trees play in the boreal hydrological cycle. Consequently, forest management practices that alter forest stand structure could have large cascading effects on the way water moves through these landscapes (Greiser et al., 2018). For instance, thinning reduces basal area and correspondingly results in a reduction in the LAI of the remaining forest stand, whereas nitrogen fertilization promotes greater aboveground carbon allocation leading to an increase in LAI in northern forested ecosystems (Lim et al., 2015). To assess how forest management practices may influence the overall magnitude of ET as well as the relative importance of the different ET flux components we ran the APES model with a range of canopy LAI values; from 1 to 7 $m^2 m^{-2}$. This resulted in an increase of total ET by *ca*. 50 mm, or 27 %, with increasing LAI (Fig. 6a). The outcome of these simulations also enabled us to identify threshold in canopy LAI where there are changes in the dominant ET flux component. For example, for sparse stands with LAI less than 3 m^2m^{-2} understory evapotranspiration is the dominant water loss pathway, whereas in forest stands with an LAI greater than 3 $m^2 m^{-2}$ transpiration becomes the dominant ET flux component. (Fig. 6b). Understanding how LAI influences total ET and its individual flux components thereby provides an opportunity to assess how different forest management practices may affect the movement of water in forested landscapes, and, in turn, could assist in the development of more sustainable management practices (Stenberg et al., 2018;Sarkkola et al., 2013a).

In conclusion, this study is unique in that it combines empirical data and a model approach to assess both the vertical and lateral fluxes of water in a northern boreal catchment. Both our empirical measurements and model estimates clearly showed that canopy trees play a central role in the water cycle of northern boreal forests, representing *ca.* 70 % of the water loss during the growing season. Forest management practices that alter forest stand structure, such as commercial thinning, continuous cover forestry, and clear cutting, are therefore likely to have large cascading effects on the way water moves through these forested landscapes. Additionally, it is important remember that this study was conducted during a single growing season, and it is reasonable to assume that changes in climatic conditions could also alter the magnitude and relative importance of different water loss pathways. Thus, further studies are needed to better understand how forest management practices and environmental conditions influence total ET and its individual flux components in order to identify more sustainable forest management practices in a changing climate.

Code and data availability

Sapflux data is archived in the sapfluxnet data base (https://github.com/sapfluxnet/sapfluxnet-public/wiki). Data on greenhouse gas, water and energy fluxes as well as meteorological and environmental data used for model forcing are available through the ICOS portal, Svartberget station (www.icos-sweden.se/station_svartberget.html). Model source code is available upon request.

Author Contributions

N.K., N.J.H., P.T., R.O., and H.L. worked on the conceptualization of the research goals. N.K., N.J.H. and P.T. installed, collected and analyzed the sapflux data; K.H. and S.L. performed the modelling; J.C and M.P. were responsible for processing the eddy covariance data; E.M.H. and J.W. provided the forest canopy data that was acquired by airborne laser scanning. N.K. and N.J.H. wrote the paper with contributions from all other others.

Acknowledgements

We thank the research staff at Svartberget and ICOS Sweden for their help in the establishment and collection of data presented in this manuscript. This work was supported by grants from the Swedish Research Council (VR, grant number, 2015-04791) and the Knut and Alice Wallenberg Foundation (grant number 2015.0047). Financial support from the

Swedish Research Council and contributing research institutes to the Swedish Integrated Carbon Observation System (ICOS-Sweden) Research Infrastructure and the Swedish Infrastructure for Ecosystem Science (SITES) are also acknowledged.

Competing interests

The authors declare that they have no conflict of interest.

References

Baldocchi, D. D., Vogel, C. A., and Hall, B.: Seasonal variation of energy and water vapor exchange rates above and below a boreal jack pine forest canopy, Journal of Geophysical Research-Atmospheres, 102, 28939-28951, 10.1029/96jd03325, 1997.

Barber, V. A., Juday, G. P., and Finney, B. P.: Reduced growth of Alaskan white spruce in the twentieth century from temperature-induced drought stress, Nature, 405, 668-673, 10.1038/35015049, 2000.

Barbier, S., Balandier, P., and Gosselin, F.: Influence of several tree traits on rainfall partitioning in temperate and boreal forests: a review, Ann. For. Sci., 66, 602, 2009.

Barnett, T. P., Adam, J. C., and Lettenmaier, D. P.: Potential impacts of a warming climate on water availability in snow-dominated regions, Nature, 438, 303-309, 10.1038/nature04141, 2005.

Bidartondo, M. I., Ek, H., Wallander, H., and Soderstrom, B.: Do nutrient additions alter carbon sink strength of ectomycorrhizal fungi?, New Phytologist, 151, 543-550, 10.1046/j.1469-8137.2001.00180.x, 2001.

Bond-Lamberty, B., Gower, S. T., Amiro, B., and Ewers, B. E.: Measurement and modelling of bryophyte evaporation in a boreal forest chronosequence, Ecohydrology, 4, 26-35, 10.1002/eco.118, 2011.

Byun, K., Chiu, C. M., and Hamlet, A. F.: Effects of 21st century climate change on seasonal flow regimes and hydrologic extremes over the Midwest and Great Lakes region of the US, Sci. Total Environ., 650, 1261-1277, 10.1016/j.scitotenv.2018.09.063, 2019.

Cavanaugh, M. L., Kurc, S. A., and Scott, R. L.: Evapotranspiration partitioning in semiarid shrubland ecosystems: a two-site evaluation of soil moisture control on transpiration, Ecohydrology, 4, 671-681, 10.1002/eco.157, 2011.

Chi, J. S., Nilsson, M. B., Kljun, N., Wallerman, J., Fransson, J. E. S., Laudon, H., Lundmark, T., and Peichl, M.: The carbon balance of a managed boreal landscape measured from a tall tower in northern Sweden, Agric. For. Meteorol., 274, 29-41, 10.1016/j.agrformet.2019.04.010, 2019.

Cienciala, E., Kučera, J., Lindroth, A., Čermák, J., Grelle, A., and Halldin, S.: Canopy transpiration from a boreal forest in Sweden during a dry year, Agric. For. Meteorol., 86, 157-167, https://doi.org/10.1016/S0168-1923(97)00026-9, 1997.

Coenders-Gerrits, A. M. J., van der Ent, R. J., Bogaard, T. A., Wang-Erlandsson, L., Hrachowitz, M., and Savenije, H. H. G.: Uncertainties in transpiration estimates, Nature, 506, E1, 10.1038/nature12925, 2014.

Constantin, J., Grelle, A., Ibrom, A., and Morgenstern, K.: Flux partitioning between understorey and overstorey in a boreal spruce/pine forest determined by the eddy covariance method, Agricultural and Forest Meteorology, 98-9, 629-643, 1999.

Domec, J.-C., Sun, G., Noormets, A., Gavazzi, M. J., Treasure, E. A., Cohen, E., Swenson, J. J., McNulty, S. G., and King, J. S.: A Comparison of Three Methods to Estimate Evapotranspiration in Two Contrasting Loblolly Pine Plantations: Age-Related Changes in Water Use and Drought Sensitivity of Evapotranspiration Components, Forest Science, 58, 497-512, 10.5849/forsci.11-051, 2012.

Eades, H. W.: Iodine as an indicator of sapwood and heartwood, The Forestry Chronicle, 13, 470-477, 10.5558/tfc13470-3, 1937.

Evaristo, J., Jasechko, S., and McDonnell, J. J.: Global separation of plant transpiration from groundwater and streamflow, Nature, 525, 91-94, 10.1038/nature14983, 2015.

Farquhar, G. D., von Caemmerer, S., and Berry, J. A.: A biochemical model of photosynthetic CO2 assimilation in leaves of C 3 species, Planta, 149, 78-90, 10.1007/bf00386231, 1980.

Ford, C. R., McGuire, M. A., Mitchell, R. J., and Teskey, R. O.: Assessing variation in the radial profile of sap flux density in Pinus species and its effect on daily water use, Tree Physiol., 24, 241-249, 10.1093/treephys/24.3.241, 2004.

Gash, J. H. C.: ANALYTICAL MODEL OF RAINFALL INTERCEPTION BY FORESTS, Quarterly Journal of the Royal Meteorological Society, 105, 43-55, 10.1002/qj.49710544304, 1979.

Githui, F., Selle, B., and Thayalakumaran, T.: Recharge estimation using remotely sensed evapotranspiration in an irrigated catchment in southeast Australia, Hydrological Processes, 26, 1379-1389, 10.1002/hyp.8274, 2012.

Good, S. P., Soderberg, K., Guan, K., King, E. G., Scanlon, T. M., and Caylor, K. K.: 2H isotopic flux partitioning of evapotranspiration over a grass field following a water pulse and subsequent dry down, Water Resources Research, 50, 1410-1432, 10.1002/2013wr014333, 2014.

Granier, A.: Evaluation of transpiration in a Douglas-Fir stand by means of sap flow measurements, Tree Physiology, 3, 309-319, 1987.

Greiser, C., Meineri, E., Luoto, M., Ehrlen, J., and Hylander, K.: Monthly microclimate models in a managed boreal forest landscape, Agricultural and Forest Meteorology, 250, 147-158, 10.1016/j.agrformet.2017.12.252, 2018.

Grelle, A., Lundberg, A., Lindroth, A., Morén, A. S., and Cienciala, E.: Evaporation components of a boreal forest: variations during the growing season, J. Hydrol., 197, 70-87, 10.1016/S0022-1694(96)03267-2, 1997.

Gu, C., Ma, J., Zhu, G., Yang, H., Zhang, K., Wang, Y., and Gu, C.: Partitioning evapotranspiration using an optimized satellite-based ET model across biomes, Agric. For. Meteorol., 259, 355-363, https://doi.org/10.1016/j.agrformet.2018.05.023, 2018.

Hamada, S., Ohta, T., Hiyama, T., Kuwada, T., Takahashi, A., and Maximov, T. C.: Hydrometeorological behaviour of pine and larch forests in eastern Siberia, Hydrol. Process., 18, 23-39, 10.1002/hyp.1308, 2004.

Harkonen, S., Lehtonen, A., Manninen, T., Tuominen, S., and Peltoniemi, M.: Estimating forest leaf area index using satellite images: comparison of k-NN based Landsat-NFI LAI with MODIS-RSR based LAI product for Finland, Boreal Environment Research, 20, 181-195, 2015.

Hernandez-Santana, V., Hernandez-Hernandez, A., Vadeboncoeur, M. A., and Asbjornsen, H.: Scaling from single-point sap velocity measurements to stand transpiration in a multispecies deciduous forest: uncertainty sources, stand structure effect, and future scenarios, Can. J. For. Res., 45, 1489-1497, 10.1139/cjfr-2015-0009, 2015.

Iida, S., Ohta, T., Matsumoto, K., Nakai, T., Kuwada, T., Kononov, A. V., Maximov, T. C., van der Molen, M. K., Dolman, H., Tanaka, H., and Yabuki, H.: Evapotranspiration from understory vegetation in an eastern Siberian boreal larch forest, Agric. For. Meteorol., 149, 1129-1139, 10.1016/j.agrformet.2009.02.003, 2009.

IPCC: Climate Change 2014: Synthesis Report. Contribution of Working Groups I, II and III to the Fifth Assessment Report of the

Intergovernmental Panel on Climate Change, Geneva, Switzerland, 151, 2014.

IPCC: An IPCC Special Report on the impacts of global warming of 1.5°C above pre-industrial levels and related global greenhouse gas emission pathways, in the context of strengthening the global response to the threat of climate change, sustainable development, and efforts to eradicate poverty, 2018.

James, S. A., Clearwater, M. J., Meinzer, F. C., and Goldstein, G.: Heat dissipation sensors of variable length for the measurement of sap flow in trees with deep sapwood, Tree Physiol., 22, 277-283, 10.1093/treephys/22.4.277, 2002.

Jasechko, S., Sharp, Z. D., Gibson, J. J., Birks, S. J., Yi, Y., and Fawcett, P. J.: Terrestrial water fluxes dominated by transpiration, Nature, 496, 347-+, 10.1038/nature11983, 2013.

Karlsen, R. H., Grabs, T., Bishop, K., Buffam, I., Laudon, H., and Seibert, J.: Landscape controls on spatiotemporal discharge variability in a boreal catchment, Water Resources Research, 52, 6541-6556, 10.1002/2016wr019186, 2016.

Kelliher, F. M., Lloyd, J., Arneth, A., Byers, J. N., McSeveny, T. M., Milukova, I., Grigoriev, S., Panfyorov, M., Sogatchev, A., Varlargin, A., Ziegler, W., Bauer, G., and Schulze, E. D.:

Evaporation from a central Siberian pine forest, J. Hydrol., 205, 279-296, http://dx.doi.org/10.1016/S0022-1694(98)00082-1, 1998.

Kieloaho, A.-J., and Launiainen, S.: Effects of functional traits of bryophyte layer on water cycling and energy balance in boreal and arctic ecosystems, EGU General Assembly Conference, 2018, 11786,

Kljun, N., Calanca, P., Rotach, M. W., and Schmid, H. P.: A simple two-dimensional parameterisation for Flux Footprint Prediction (FFP), Geosci. Model Dev., 8, 3695-3713, 10.5194/gmd-8-3695-2015, 2015.

Kool, D., Agam, N., Lazarovitch, N., Heitman, J. L., Sauer, T. J., and Ben-Gal, A.: A review of approaches for evapotranspiration partitioning, Agric. For. Meteorol., 184, 56-70, 10.1016/j.agrformet.2013.09.003, 2014.

Koster, R. D., and Milly, P. C. D.: The interplay between transpiration and Runoff formulations in land surface schemes used with atmospheric models, J. Clim., 10, 1578-1591, 1997.

Kulmala, L., Pumpanen, J., Kolari, P., Muukkonen, P., Hari, P., and Vesala, T.: Photosynthetic production of ground vegetation in different-aged Scots pine (Pinus sylvestris) forests, Canadian Journal of Forest Research-Revue Canadienne De Recherche Forestiere, 41, 2020-2030, 10.1139/x11-121, 2011.

Laudon, H., Taberman, I., Agren, A., Futter, M., Ottosson-Lofvenius, M., and Bishop, K.: The Krycklan Catchment Study-A flagship infrastructure for hydrology, biogeochemistry, and climate research in the boreal landscape, Water Resources Research, 49, 7154-7158, 10.1002/wrcr.20520, 2013.

Launiainen, S., Rinne, J., Pumpanen, J., Kulmala, L., Kolari, P., Keronen, P., and Vesala, T.: Eddy covariance measurements of CO, Boreal Environment Research, 569-588, 2005.

Launiainen, S.: Seasonal and inter-annual variability of energy exchange above a boreal Scots pine forest, Biogeosciences, 7, 3921-3940, 10.5194/bg-7-3921-2010, 2010.

Launiainen, S., Katul, G. G., Lauren, A., and Kolari, P.: Coupling boreal forest CO2, H2O and energy flows by a vertically structured forest canopy – Soil model with separate bryophyte layer, Ecological Modelling, 312, 385-405, https://doi.org/10.1016/j.ecolmodel.2015.06.007, 2015.

Lim, H., Oren, R., Palmroth, S., Tor-ngern, P., Morling, T., Nasholm, T., Lundmark, T., Helmisaari, H. S., Leppalammi-Kujansuu, J., and Linder, S.: Inter-annual variability of precipitation constrains the production response of boreal Pinus sylvestris to nitrogen fertilization, Forest Ecology and Management, 348, 31-45, 10.1016/j.foreco.2015.03.029, 2015.

Linhoss, A. C., and Siegert, C. M.: A comparison of five forest interception models using global sensitivity and uncertainty analysis, J. Hydrol., 538, 109-116, http://dx.doi.org/10.1016/j.jhydrol.2016.04.011, 2016.

https://doi.org/10.5194/hess-2019-541
Preprint. Discussion started: 24 October 2019

Lu, P., Muller, W. J., and Chacko, E. K.: Spatial variations in xylem sap flux density in the trunk of orchard-grown, mature mango trees under changing soil water conditions, Tree Physiol., 20, 683-692, 2000.

Ma, Z. H., Peng, C. H., Zhu, Q. A., Chen, H., Yu, G. R., Li, W. Z., Zhou, X. L., Wang, W. F., and Zhang, W. H.: Regional drought-induced reduction in the biomass carbon sink of Canada's boreal forests, Proceedings of the National Academy of Sciences of the United States of America, 109, 2423-2427, 10.1073/pnas.1111576109, 2012.

Marklund, L. G.: Biomassafunktioner för tall, gran och björk i Sverige, Sveriges lantbruksuniversitet, Institutionen för skogstaxering, 1988.

Maximov, T., Ohta, T., and Dolman, A. J.: Water and energy exchange in East Siberian forest: A synthesis, Agric. For. Meteorol., 148, 2013-2018, 10.1016/j.agrformet.2008.10.004, 2008.

McGaughey, R. J.: FUSION/LDV: Software for LIDAR Data Analysis and Visualization. February 2012 – FUSION Version 3.01., in, United States Department of Agriculture, Forest Service, 2012.

Medlyn, B. E., Duursma, R. A., Eamus, D., Ellsworth, D. S., Prentice, I. C., Barton, C. V. M., Crous, K. Y., De Angelis, P., Freeman, M., and Wingate, L.: Reconciling the optimal and empirical approaches to modelling stomatal conductance, Glob. Change Biol., 17, 2134-2144, doi:10.1111/j.1365-2486.2010.02375.x, 2011.

Mitchell, P. J., Veneklaas, E., Lambers, H., and Burgess, S. S. O.: Partitioning of evapotranspiration in a semi-arid eucalypt woodland in south-western Australia, Agric. For. Meteorol., 149, 25-37, https://doi.org/10.1016/j.agrformet.2008.07.008, 2009.

Näslund, M.: Skogsförsöksanstaltens gallringsförsök i tallskog, in: Meddelanden från Statens skogsförsöksanstalt, 29:1, 1936.

Odin, H.: Climate and conditions in forest soils during winter and spring at Svartberget Experimental Forest Station, Swedish University of Agricultural sciences, Uppsala, 50, 1992.

Ohta, T., Hiyama, T., Tanaka, H., Kuwada, T., Maximov, T. C., Ohata, T., and Fukushima, Y.: Seasonal variation in the energy and water exchanges above and below a larch forest in eastern Siberia, Hydrol. Process., 15, 1459-1476, 10.1002/hyp.219, 2001.

Oishi, A. C., Oren, R., and Stoy, P. C.: Estimating components of forest evapotranspiration: A footprint approach for scaling sap flux measurements, Agricultural and Forest Meteorology, 148, 1719-1732, 10.1016/j.agrformet.2008.06.013, 2008.

Oishi, A. C., Hawthorne, D. A., and Oren, R.: Baseliner: An open-source, interactive tool for processing sap flux data from thermal dissipation probes, SoftwareX, 5, 139-143, https://doi.org/10.1016/j.softx.2016.07.003, 2016.

Oki, T., and Kanae, S.: Global Hydrological Cycles and World Water Resources, Science, 313, 1068-1072, 10.1126/science.1128845, 2006.

Oren, R., Phillips, N., Ewers, B. E., Pataki, D. E., and Megonigal, J. P.: Sap-flux-scaled transpiration responses to light, vapor pressure deficit, and leaf area reduction in a flooded Taxodium distichum forest, Tree Physiol., 19, 337-347, 1999.

Palmroth, S., Bach, L. H., Nordin, A., and Palmqvist, K.: Nitrogen-addition effects on leaf traits and photosynthetic carbon gain of boreal forest understory shrubs, Oecologia, 175, 457-470, 10.1007/s00442-014-2923-9, 2014.

Peel, M. C., McMahon, T. A., and Finlayson, B. L.: Vegetation impact on mean annual evapotranspiration at a global catchment scale, Water Resources Research, 46, 16, 10.1029/2009wr008233, 2010.

Peng, C. H., Ma, Z. H., Lei, X. D., Zhu, Q., Chen, H., Wang, W. F., Liu, S. R., Li, W. Z., Fang, X. Q., and Zhou, X. L.: A drought-induced pervasive increase in tree mortality across Canada's boreal forests, Nature Climate Change, 1, 467-471, 10.1038/nclimate1293, 2011.

Phillips, N., Oren, R., and Zimmermann, R.: Radial patterns of xylem sap flow in non-, diffuse- and ring-porous tree species, Plant, Cell & Environment, 19, 983-990, 10.1111/j.1365-3040.1996.tb00463.x, 1996.

Phillips, N., and Oren, R.: A comparison of daily representations of canopy conductance based on two conditional time-averaging methods and the dependence of daily conductance on environmental factors, Annales Des Sciences Forestieres, 55, 217-235, 10.1051/forest:19980113, 1998.

Richardson, A. D., and Hollinger, D. Y.: A method to estimate the additional uncertainty in gap-filled NEE resulting from long gaps in the CO2 flux record, Agric. For. Meteorol., 147, 199-208, 10.1016/j.agrformet.2007.06.004, 2007.

Rutter, A. J., Kershaw, K. A., Robins, P. C., and Morton, A. J.: A predictive model of rainfall interception in forests, 1. Derivation of the model from observations in a plantation of Corsican pine, Agricultural Meteorology, 9, 367-384, https://doi.org/10.1016/0002-1571(71)90034-3, 1971.

Sarkkola, S., Nieminen, M., Koivusalo, H., Lauren, A., Ahti, E., Launiainen, S., Nikinmaa, E., Marttila, H., Laine, J., and Hokka, H.: Domination of growing-season evapotranspiration over runoff makes ditch network maintenance in mature peatland forests questionable, Mires and Peat, 11, 11, 2013a.

Sarkkola, S., Nieminen, M., Koivusalo, H., Lauren, A., Ahti, E., Launiainen, S., Nikinmaa, E., Marttila, H., Laine, J., and Hokka, H.: Domination of growing-season evapotranspiration over runoff makes ditch network maintenance in mature peatland forests questionable, Mires and Peat, 11, Article 2, 2013b.

Schlesinger, W. H., and Jasechko, S.: Transpiration in the global water cycle, Agric. For. Meteorol., 189-190, 115-117, https://doi.org/10.1016/j.agrformet.2014.01.011, 2014.

Selin, L.: Modeling LAI using remote sensing data sources, Institutionen för skoglig resurshushållning, Sveriges lantbruksuniversitet, 2019.

Silva, L. C. R., Anand, M., and Leithead, M. D.: Recent Widespread Tree Growth Decline Despite Increasing Atmospheric CO2, Plos One, 5, 7, 10.1371/journal.pone.0011543, 2010.

Stenberg, L., Haahti, K., Hokka, H., Launiainen, S., Nieminen, M., Lauren, A., and Koivusalo, H.: Hydrology of Drained Peatland Forest: Numerical Experiment on the Role of Tree Stand Heterogeneity and Management, Forests, 9, 19, 10.3390/f9100645, 2018.

Stenberg, P., Linder, S., Smolander, H., and Flowerellis, J.: Performance of the LAI-2000 plant canopy analyzer in estimating leaf-area index of some Scots Pine stands, Tree Physiology, 14, 981-995, 10.1093/treephys/14.7-8-9.981, 1994.

Steppe, K., De Pauw, D. J. W., Doody, T. M., and Teskey, R. O.: A comparison of sap flux density using thermal dissipation, heat pulse velocity and heat field deformation methods, Agric. For. Meteorol., 150, 1046-1056, 10.1016/j.agrformet.2010.04.004, 2010.

Stoy, P. C., Katul, G. G., Siqueira, M. B. S., Juang, J.-Y., Novick, K. A., Mccarthy, H. R., Christopher Oishi, A., Uebelherr, J. M., Kim, H.-S., and Oren, R.: Separating the effects of climate and vegetation on evapotranspiration along a successional chronosequence in the southeastern US, Glob. Change Biol., 12, 2115-2135, 10.1111/j.1365-2486.2006.01244.x, 2006.

Stoy, P. C., El-Madany, T., Fisher, J. B., Gentine, P., Gerken, T., Good, S. P., Liu, S., Miralles, D. G., Perez-Priego, O., Skaggs, T. H., Wohlfahrt, G., Anderson, R. G., Jung, M., Maes, W. H., Mammarella, I., Mauder, M., Migliavacca, M., Nelson, J. A., Poyatos, R., Reichstein, M., Scott, R. L., and Wolf, S.: Reviews and syntheses: Turning the challenges of partitioning ecosystem evaporation and transpiration into opportunities, Biogeosciences Discuss., 2019, 1-47, 10.5194/bg-2019-85, 2019.

Sun, H. Z., Aubrey, D. P., and Teskey, R. O.: A simple calibration improved the accuracy of the thermal dissipation technique for sap flow measurements in juvenile trees of six species, Trees-Struct. Funct., 26, 631-640, 10.1007/s00468-011-0631-1, 2012.

Sutanto, S. J., van den Hurk, B., Dirmeyer, P. A., Seneviratne, S. I., Röckmann, T., Trenberth, K. E., Blyth, E. M., Wenninger, J., and Hoffmann, G.: HESS Opinions "A perspective on isotope versus non-isotope approaches to determine the contribution of transpiration to total evaporation", Hydrol. Earth Syst. Sci., 18, 2815-2827, 10.5194/hess-18-2815-2014, 2014.

Suzuki, K., Kubota, J., Yabuki, H., Ohata, T., and Vuglinsky, V.: Moss beneath a leafless larch canopy: influence on water and energy balances in the southern mountainous taiga of eastern Siberia, Hydrol. Process., 21, 1982-1991, 10.1002/hyp.6709, 2007.

Tahvanainen, T., and Forss, E.: Individual tree models for the crown biomass distribution of Scots pine, Norway spruce and birch in Finland, Forest Ecology and Management, 255, 455-467, https://doi.org/10.1016/j.foreco.2007.09.035, 2008.

Tateishi, M., Kumagai, T., Utsumi, Y., Umebayasi, T., Shiiba, Y., Inoue, K., Kaji, K., Cho, K., and Otsuki, K.: Spatial variations in xylem sap flux density in evergreen oak trees with radial-porous wood: comparisons with anatomical observations, Trees-Struct. Funct., 22, 23-30, 10.1007/s00468-007-0165-8, 2008.

Telmer, K., and Veizer, J.: Isotopic constraints on the transpiration, evaporation, energy, and gross primary production Budgets of a large boreal watershed: Ottawa River Basin, Canada, Global Biogeochemical Cycles, 14, 149-165, doi:10.1029/1999GB900078, 2000.

Tor-Ngern, P., Oren, R., Oishi, A. C., Uebelherr, J. M., Palmroth, S., Tarvainen, L., Ottosson-Lofvenius, M., Linder, S., Domec, J. C., and Nasholm, T.: Ecophysiological variation of transpiration of pine forests: synthesis of new and published results, Ecological Applications, 27, 118-133, 10.1002/eap.1423, 2017.

Wang, D., Wang, G., and Anagnostou, E. N.: Evaluation of canopy interception schemes in land surface models, Journal of Hydrology, 347, 308-318, https://doi.org/10.1016/j.jhydrol.2007.09.041, 2007.

Wang, H., Tetzlaff, D., Dick, J. J., and Soulsby, C.: Assessing the environmental controls on Scots pine transpiration and the implications for water partitioning in a boreal headwater catchment, Agric. For. Meteorol., 240-241, 58-66, https://doi.org/10.1016/j.agrformet.2017.04.002, 2017.

Wang, S., Grant, R. F., Verseghy, D. L., and Andrew Black, T.: Modelling carbon-coupled energy and water dynamics of a boreal aspen forest in a general circulation model land surface scheme, Int. J. Climatol., 22, 1249-1265, 10.1002/joc.776, 2002.

Warren, R. K., Pappas, C., Helbig, M., Chasmer, L. E., Berg, A. A., Baltzer, J. L., Quinton, W. L., and Sonnentag, O.: Minor contribution of overstorey transpiration to landscape evapotranspiration in boreal permafrost peatlands, Ecohydrology, 11, 10, 10.1002/eco.1975, 2018.

Watanabe, T., and Mizutani, K.: Model study on micrometeorological aspects of rainfall interception over an evergreen broad-leaved forest, Agric. For. Meteorol., 80, 195-214, https://doi.org/10.1016/0168-1923(95)02301-1, 1996.

Wei, Z., Yoshimura, K., Wang, L., Miralles, D. G., Jasechko, S., and Lee, X.: Revisiting the contribution of transpiration to global terrestrial evapotranspiration, Geophysical Research Letters, 44, 2792-2801, 10.1002/2016GL072235, 2017.

Wharton, S., Schroeder, M., Paw U, K. T., Falk, M., and Bible, K.: Turbulence considerations for comparing ecosystem exchange over old-growth and clear-cut stands for limited fetch and complex canopy flow conditions, Agric. For. Meteorol., 149, 1477-1490, https://doi.org/10.1016/j.agrformet.2009.04.002, 2009.

Wutzler, T., Lucas-Moffat, A., Migliavacca, M., Knauer, J., Sickel, K., Šigut, L., Menzer, O., and Reichstein, M.: Basic and extensible post-processing of eddy covariance flux data with REddyProc, Biogeosciences, 15, 5015-5030, 10.5194/bg-15-5015-2018, 2018.

Zeng, N., Shuttleworth, J. W., and Gash, J. H. C.: Influence of temporal variability of rainfall on interception loss. Part I. Point analysis, J. Hydrol., 228, 228-241, 10.1016/s0022-1694(00)00140-2, 2000.

Zhao, W., and Qualls, R. J.: A multiple-layer canopy scattering model to simulate shortwave radiation distribution within a homogeneous plant canopy, Water Resources Research, 41, doi:10.1029/2005WR004016, 2005.

Zhao, W., and Qualls, R. J.: Modeling of long-wave and net radiation energy distribution within a homogeneous plant canopy via multiple scattering processes, Water Resources Research, 42, doi:10.1029/2005WR004581, 2006.

Ågren, A. M., Haei, M., Blomkvist, P., Nilsson, M. B., and Laudon, H.: Soil frost enhances stream dissolved organic carbon concentrations during episodic spring snow melt from boreal mires, Glob. Change Biol., 18, 1895-1903, 10.1111/j.1365-2486.2012.02666.x, 2012.

Öquist, M. G., Bishop, K., Grelle, A., Klemedtsson, L., Köhler, S. J., Laudon, H., Lindroth, A., Ottosson-Löfvenius, M., Wallin, M. B., and Nilsson, M. B.: The Full Annual Carbon Balance of Boreal Forests Is Highly Sensitive to Precipitation, Environmental Science & Technology Letters, 1, 315-319, 10.1021/ez500169j, 2014.